

Article

# Analysis of the Effect of the Variable Charging Current Control Method on Cycle Life of Li-ion Batteries

In-Ho Cho <sup>1,\*</sup>, Pyeong-Yeon Lee <sup>2</sup> and Jong-Hoon Kim <sup>2,\*</sup>

<sup>1</sup> Smart Electrical & Signaling Division, Korea Railroad Research Institute, Uiwang-si 16105, Korea

<sup>2</sup> Department of Electrical Engineering, Chungnam National University, Daejeon 34134, Korea

\* Correspondence: inhocho@krii.re.kr (I.-H.C.); whdgns0422@cnu.ac.kr (J.-H.K.);

Tel.: +82-31-460-5469 (I.-H.C.); +82-42-821-5657 (J.-H.K.)

Received: 28 May 2019; Accepted: 1 August 2019; Published: 6 August 2019



**Abstract:** Applications of rechargeable batteries have recently expanded from small information technology (IT) devices to a wide range of other industrial sectors, including vehicles, rolling stocks, and energy storage system (ESS), as a part of efforts to reduce greenhouse gas emissions and enhance convenience. The capacity of rechargeable batteries adopted in individual products is meanwhile increasing and the price of the batteries in such products has become an important factor in determining the product price. In the case of electric vehicles, the price of batteries has increased to more than 40% of the total product cost. In response, various battery management technologies are being studied to increase the service life of products with large-capacity batteries and reduce maintenance costs. In this paper, a charging algorithm to increase the service life of batteries is proposed. The proposed charging algorithm controls charging current in anticipation of heating inside the battery while the battery is being charged. The validity of the proposed charging algorithm is verified through an experiment to compare charging cycles using high-capacity type lithium-ion cells and high-power type lithium-ion cells.

**Keywords:** battery charging; cycle-life; state-of-health (SOH); battery cycle-life extension

## 1. Introduction

The trend of wider diffusion of mobile electronics, such as mobile phones and laptops, and the increasing demand for high performance devices have led to growth of both the battery industry and the information technology (IT) industry. Consumers need mobile devices that can be used for long periods of time on a single charge, even with short battery charging time. This has motivated research on rapid charging technology and improving the energy density of batteries. Furthermore, the growth of the electric vehicle (EV) market has given rise to the new issue in the battery industry of managing the battery's state-of-health (SOH). Unlike small mobile devices, which are often replaced within two to three years, EVs are relatively expensive products and their batteries, which generally have a life expectancy of more than eight years, account for the largest cost among all parts. As a result, batteries in the automotive industry must be capable of maintaining battery capacity for a considerable period of time, and many studies have been conducted to manage the battery's SOH.

The cycle life of batteries that generate electricity through chemical reactions is determined by various external factors [1–8]. First, battery charging operation in low temperature conditions reduces the chemical reaction rate of lithium ions. This causes the accumulation of lithium-ion metals in the anode layer, which reduces the capacity and in turn is directly linked to the battery's lifetime [1]. Second, high C-rate charging and high depth of discharge (DOD) range result in loss of active material

and the formation of a thick layer of solid electrolyte interphase (SEI) at the surface of electrodes. This increases internal impedance and reduces the capacity of the battery [2,3]. Third, overcharge battery operation causes unwanted heating inside the battery. This results in cracking of the SEI and loss of active area inside the battery, which reduces the total capacity of the battery [4,5]. Fourth, over-discharge of batteries also reduces the number of ions participating in electrochemical reaction, which causes capacity loss [4]. Fifth, battery cycle life can be shortened by charging/discharging operation at high temperatures. Electrolytes and the binders of the battery are destroyed during the charging/discharging operation at high temperatures and this reduces the capacity of the batteries [6,7]. In addition to the aforementioned reasons, the battery SOH is affected by various factors and many of these factors are related to the charging conditions. Thus, the aging of batteries can be mitigated by developing the charging algorithm.

Recently, various battery charging algorithms have been investigated to extend the battery cycle life and reduce restrictions on battery use [7–19]. Most of these studies focused on developing charging algorithms and profiles to reduce the battery charging time by adopting a high C-rate current. One of the most common fast charging algorithms is the CC-CV, constant current-constant voltage, charging method [8,9]. Batteries are charged with constant current until the maximum acceptable battery voltage is reached; after that charging is continued with a fixed charging voltage, and charging is completed when the charging current reaches a preset small value. The multi-stage constant current (MCC) charging method is another well-known fast charging method. Unlike the constant-current charging method, charging current is divided into several levels in the MCC method to reduce the charging time and heat generated inside the battery during charging [8,13]. Generally, the charging current is controlled in a direction where the size of the charging current decreases as the charging time progresses. The constant power (CP) charging method maintains charging power during the charging operation [7]. High charging current is induced at the beginning of charging and it is gradually decreased as the battery voltage increases. The boost charging method is also one of the basic fast charging methods based on the CC-CV charging profile [8,17]. It adopts a high current charging period at the beginning of the CC-CV charging profile to reduce the charging time. Figure 1 shows the various battery charging profiles.

Although various fast charging technologies are being studied through many different approaches to reduce the charging time while minimizing capacity loss, they cannot reflect the characteristics of changes in internal impedance, which depends on changes in state-of-charge (SOC) or SOH. As a result, the battery's life expectancy, which is determined by the available power rating and total remaining capacity, is rapidly deteriorated with use of the fast charging method. Therefore, the conventional CC-CV charging profiles are still widely utilized in applications where the battery price is a significant factor in relation to the overall price and/or the battery's characteristics have a significant impact on the performance of the product.

In this paper, the aging characteristics of the battery with use of the CC-CV method are analyzed and a new charging method that minimizes battery degradation is proposed. The proposed method controls the charging current by considering the difference in internal impedance caused by SOC changes in order to minimize the heating of the battery during charging. To verify the effectiveness of the proposed charging method, the battery aging characteristics when the proposed charging method is applied are compared with those observed with use of the CC-CV method.

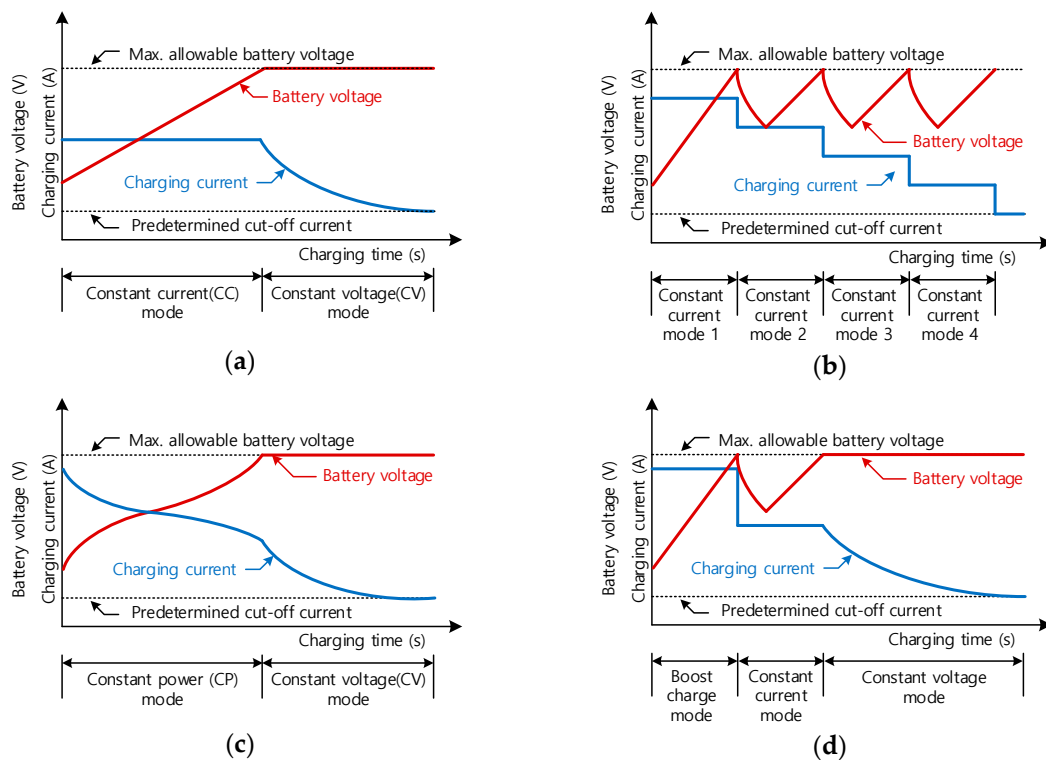


**Figure 1.** Battery charging profiles: (a) Constant current-constant voltage (CC-CV) charging method; (b) Multi-stage constant current (MCC) charging method; (c) Constant power (CP) charging method; (d) Boost charging method.

## 2. Equivalent Circuit Model for SOH Estimation

Various physical and chemical changes occur within the battery as battery cells age [20–25]. Physically, the structure of electrodes is changed and this reduces the capacity of the battery; chemically, the loss of active material causes capacity reduction, and unwanted chemical reactions within the electrolyte prevent circulation of internal active ions. These aging characteristics typically result in a change in electrical properties, such as reduced capacity of the battery or increased internal resistance ( $R_{int.}$ ), which in turn undermines the output power characteristics of the battery.

Figure 2 shows the conventional equivalent circuit model (ECM), which is widely used in the electrical analysis of batteries. SOH estimation using the ECM offers the advantage of a relatively simple calculation while expressing the change in characteristics of the battery. The characteristics of batteries are explained in the ECM by the open circuit voltage (OCV), which represents the battery capacity, the internal ohmic resistance ( $R_i$ ), which denotes the resistance of the electrolyte, and the internal diffusion resistance ( $R_{diff.}$ )-capacitance ( $C_{diff.}$ ) network, which represents the charge diffusion/transfer characteristics. The applied voltages to  $R_i$  and  $R_{diff.}$ - $C_{diff.}$  network are represented as  $V_{ohmic}$  and  $V_{diff.}$ , respectively.  $V_{BATT}$  in Figure 2 shows the voltage across the terminals of a battery. The characteristics of batteries that vary with the SOC and SOH can be expressed through changes in the internal resistance, which is determined by the sum of  $R_i$  and  $R_{diff.}$ , and capacitance values in the ECM [20]. Therefore, for accurate prediction of the operating characteristics and SOH of batteries using the equivalent circuit model, it is necessary to clearly identify the variation in the internal resistance parameters according to the condition of the battery and to measure the parameters of the equivalent circuit periodically. Figure 3 illustrates the hybrid pulse power characterization (HPPC) method for measuring the resistances in the ECM. The HPPC method obtains the internal parameters of the ECM by monitoring the change in the internal voltage of the battery while varying the charge current and discharge current within the range of operation of the battery [26,27].

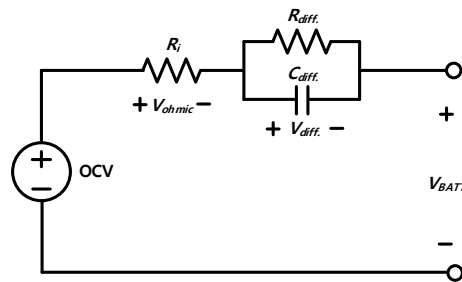


Figure 2. Configuration of the equivalent circuit model.

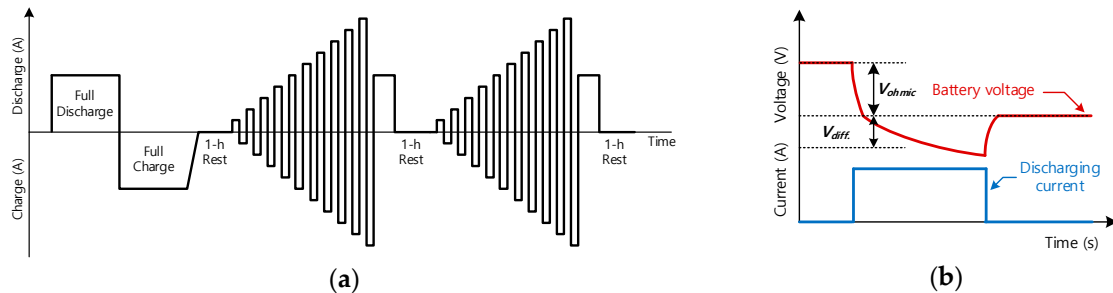


Figure 3. Hybrid pulse power characterization (HPPC) parameter calculation method: (a) Charging-discharging profile; (b) Parameters estimation method.

### 3. Effect of Internal Heat on SOH of Batteries

A number of factors affect battery aging including temperature inside/outside the battery, SOC, depth of discharge (DOD), etc., [4]. Among these, temperature, which has a direct effect on the rate of chemical reaction of batteries, is one of the most influential factors in the aging of batteries. According to the Arrhenius Equation (1), which describes a chemical reaction, the rate of chemical reaction and temperature have a linear relationship of logarithmic scale. Therefore, in the case of batteries, which charge and discharge energy through chemical reactions, temperature management is considered to have a significant effect on battery aging.

$$r = A \times e^{\left(\frac{E_a}{kT}\right)}, \quad (1)$$

where  $r$  is the reaction rate,  $k$  is Boltzmann's constant,  $A$  is the frequency factor,  $E_a$  is the activation energy, and  $T$  is the absolute temperature.

### 4. Proposed Charging Method for Minimizing Battery Degradation

As mentioned earlier, the life cycle estimation method using equivalent circuit models is widely employed in many applications due to its advantages of being simple and quite accurate in calculation [28]. The internal resistances in the equivalent circuit are measured periodically using the HPPC test method and the measured values of an aged battery cell are compared with those of a fresh cell, and the differences in the parameter values are used to calculate the life of the battery. This paper proposes a variable battery charging current algorithm (VCC) that controls the charging current in a way that minimizes heating inside the battery when charging. This is done using the characteristics of internal resistance change in batteries, which depend on the SOC and the relationship between heating and aging of the battery.

Figure 4 shows the measured internal resistance values of batteries in accordance with the SOC at intervals of 10 cycles using INR 18650 25R cells of Samsung SDI (Yongin-si, Korea). As shown in Figure 4, the internal resistance of a battery varies significantly with the SOC and the life cycle. In particular, the Figure 4 shows that changes in internal resistance do not have a linear relationship with changes in the SOC. The internal resistance shows a proportional decrease in the resistance to

the SOC in the range where the SOC decreases from 100% to 40%, whereas below 40% it shows an increase in resistance as opposed to SOC reduction, as can be seen in Figure 4. Given that heating inside the battery is ultimately determined by the value of the current flowing into the resistor, it can be expected that the temperature of the battery will continue to change during the charging process and heat generation will increase in the low and high SOC range, if the CC-CV method, which is the most popular battery charging algorithm, is applied. Therefore, this paper proposes a variable charging current algorithm that changes the amount of charging current according to the SOC, taking into account the internal resistance of the battery in order to slow the aging of battery cells according to the charging power. The proposed charging algorithm is a method to minimize internal thermal variation of the battery in the charging process and thereby prevent fluctuation of the charging power loss ( $P_{Loss}$ ), which directly affects the heating of the battery while the battery is being charged. Since the internal resistance of a battery generally shows characteristics that vary with the SOC condition, a method of controlling the charging current of the battery according to the changing resistance value is required, and the charging current value ( $I_{Charge}$ ) is achieved using Equation (2) in the present study. To verify the effectiveness of the proposed charging algorithm, two types of batteries, high-capacity lithium-ion cells (INR 25R) and high-power lithium-ion cells (INR 29E), were compared with use of the conventional CC-CV charging method and the proposed VCC method.

$$P_{Loss}(W) = I_{Charge}^2 \times R_{int.}, \quad I_{Charge}(A) = \sqrt{P_{Loss}/R_{int.}} \quad (2)$$

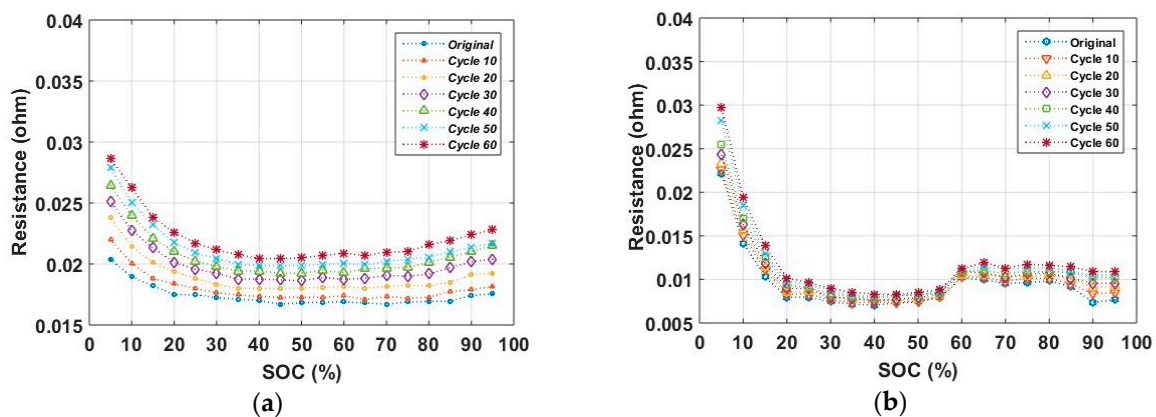


**Figure 4.** Measured internal resistance of INR 25R battery as it aged: (a) Internal ohmic resistance,  $R_i$ ; (b) Internal diffusion resistance,  $R_{diff}$ .

## 5. Experimental Configuration of the Proposed Algorithm

Two different types of batteries were used in the experiment: a battery with a high output power characteristic, INR 25R, which is composed of nickel cobalt aluminum oxide (NCA) and a battery with a high energy density characteristic, INR 29E, which is composed of nickel manganese cobalt oxide (NMC). Table 1 presents detailed specifications of each battery. The experiment was conducted in a temperature chamber set to be maintained at a temperature of 25 °C and the experiment proceeded as follows.

**Table 1.** Specifications of batteries used in the experiment.

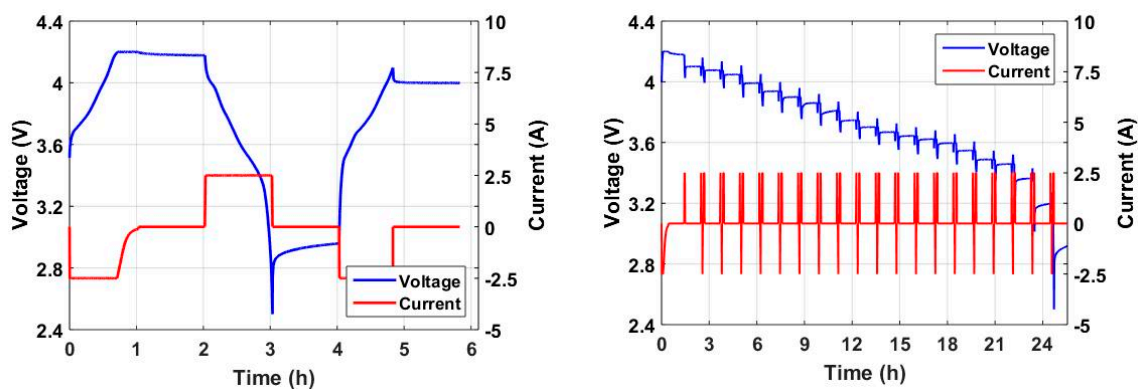
Characteristics	INR 25R	INR 29E
Rated voltage	3.60 V	3.65 V
Maximum continuous discharge current	20 A	2.750 A
Rated capacity	2500 mAh	2750 mAh
Cut-off voltage	4.20 V (Charge) 2.50 V (Discharge)	4.20 V (Charge) 2.50 V (Discharge)
Materials	C (Negative) LiCoNiAlO <sub>2</sub> (NCA)	C (Negative) LiNiMnCoO <sub>2</sub> (NMC)

Step 1: Measure the exact capacity of each battery.

To measure the capacity of the battery, first it was fully charged up to 4.2 V using the CC-CV charging method using 0.5 C charging current. A 0.5 C discharge current was then applied to discharge the battery to the cut-off voltage and the capacity of the battery was calculated using the discharge time. After each capacity calculation process, one hour of rest time was given to the battery to complete the internal chemistry reaction.

Step 2: Measure the internal resistance of the battery.

The HPPC test method was applied to measure the internal resistance of the battery using 0.5 C charging/discharging current. The resistance was measured by lowering the SOC by increments of 5% from 100%. Figure 5 shows the experimental procedure used to measure the internal resistance.

**Figure 5.** Experimental procedure used to measure the internal resistance.

Step 3: Derive the charging current.

Charging current values for each SOC were derived in this step using the resistance values obtained from the previous step. In order to maintain a constant amount of heat inside the battery generated during the charging process, a constant value of charging loss was set and the charging current was calculated. Considering the tendency of the internal resistance of the battery to increase as the SOC becomes lower, the loss value when 0.5 C charging is applied was taken as the reference value at 50% of the SOC. Table 2 shows the charging current and internal resistance at each SOC. Only the DC internal resistance (DCIR), which indicates the effect of DC current on the battery is considered in calculating the charging current. The resistance is widely used value when comparing the performance of the battery and also has the characteristics of large variation on the SOC [29–31].

**Table 2.** Measured internal resistance and calculated charging current in the experiment.

SOC (%)	INR 25R (NCA)		INR 29E (NMC)	
	DCIR (ohm)	Current (A)	DCIR (ohm)	Current (A)
100	0.0252	1.2258	0.0349	1.3991
95	0.0252	1.2327	0.0349	1.3991
90	0.0248	1.2431	0.0349	1.3988
85	0.0261	1.2111	0.0364	1.3693
80	0.0268	1.1962	0.0380	1.3412
75	0.0265	1.2015	0.0384	1.3334
70	0.0262	1.2084	0.0377	1.3468
65	0.0268	1.1963	0.0379	1.3429
60	0.0271	1.1893	0.0388	1.3276
55	0.0248	1.2433	0.0384	1.3334
50	0.0242	1.2570	0.0356	1.3861
45	0.0240	1.2632	0.0349	1.3991
40	0.0241	1.2619	0.0344	1.4101
35	0.0243	1.2555	0.0343	1.4102
30	0.0247	1.2464	0.0348	1.4010
25	0.0254	1.2269	0.0351	1.3947
20	0.0255	1.2268	0.0356	1.3859
15	0.0285	1.1589	0.0367	1.3649
10	0.0331	1.0757	0.0400	1.3073
5	0.0425	0.9492	0.0473	1.2012
0	0.0425	0.9439	0.0473	1.2012

Step 4: Aging test using the VCC method.

The battery aging experiment was carried out by repeating the charging cycle using the charging current value obtained in Step 3. The SOH of the battery was checked by measuring the internal resistance of the battery at every 10 charging–discharging cycles.

To compare the aging of batteries according to the charging method, the degree of aging of the batteries with application of the existing CC-CV charging method was measured using the same two types of batteries as applied during the VCC algorithm aging test. The battery aging condition was compared after 60 cycles of the charging test were carried out in different ways to compare the degree of aging according to the charging algorithm.

## 6. Experimental Results

Figure 6 shows the results of measuring the internal resistance variation of the battery by the SOC according to each charging method by applying the proposed VCC method and the conventional CC-CV charging method. The battery charging with the VCC method shows less variation in internal resistance, and this is more visible in high-power battery cells. The difference in the increase in resistance of a battery resulting from the batteries having different charging algorithms can be seen, similarly to the tendency of capacity reduction due to the aging of the battery. Figure 7 shows the variation of the capacity of each battery as the charging cycle repeats and Table 3 shows the comparison result of the capacity degradation rate on each method. As shown in this Figure 7, there is less capacity change in the battery cell with the proposed charging algorithm. Figure 8 shows the results of the change in charging time following the aging test. In the proposed method, a resistance value at a 50% SOC, which has the lowest internal resistance, and a current value of 0.5 C were used to obtain the charging power loss, and the power loss value is used to calculate the charging current due to the change in resistance. As a result, as the test progresses, the difference in charging time was reduced or reversed depending on the battery type because the charging time is longer with the proposed charging method than with the conventional CC-CV charging method at the beginning of the charging test, but with aging this difference becomes smaller. This is ascribed to a slower aging process and

smaller internal resistance characteristics in the proposed charging algorithm when compared to the conventional method of charging [32].

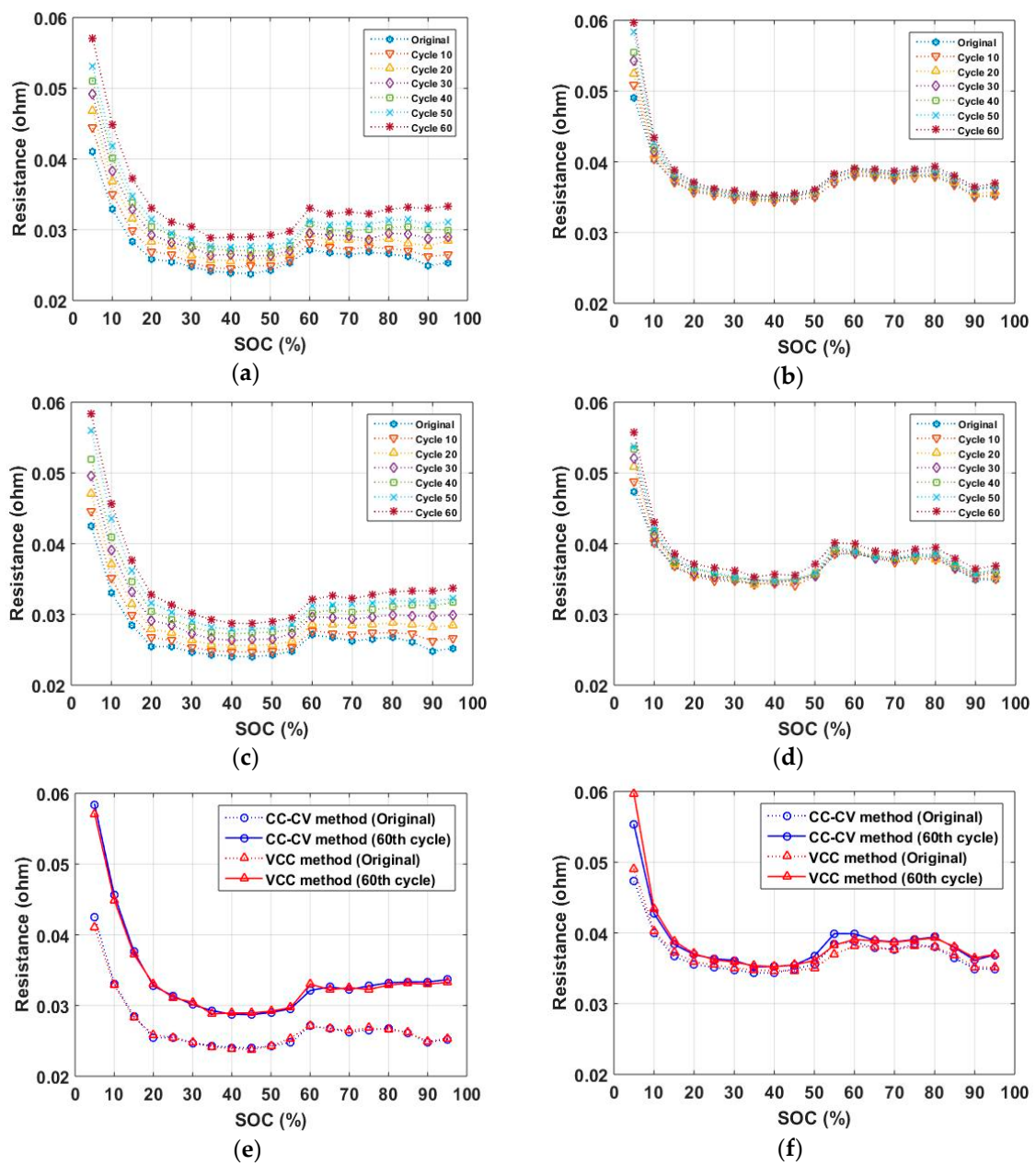


**Figure 6.** Hybrid pulse power characterization (HPPC) parameter calculation method: (a) DCIR of cell with NCA material (CC-CV); (b) DCIR of cell with NMC material (CC-CV); (c) DCIR of cell with NCA material (VCC); (d) DCIR of cell with NMC material (VCC); (e) comparison of internal resistance (NCA); (f) comparison of internal resistance (NMC).

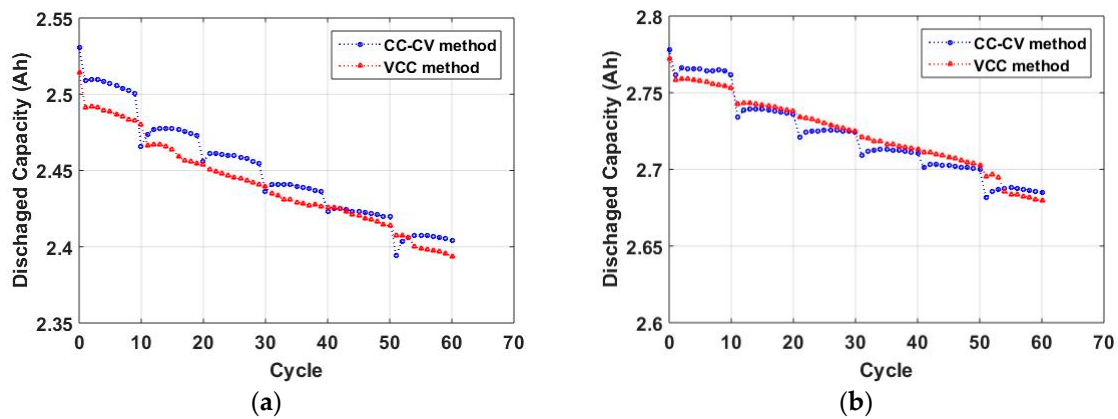


Figure 7. The discharging capacity by cycle number: (a) cell with NCA material; (b) cell with NMC material.

Table 3. Comparison of the capacity degradation rate.

Battery Types and Cycles		CC-CV Method		VCC Method	
		Capacity (Ah)	Growth Rate (%)	Capacity (Ah)	Growth Rate (%)
25R (NCA)	Original	2.5303	−4.993	2.5143	−4.804
	60th cycle	2.4039		2.3935	
29E (NMC)	Original	2.7781	−3.353	2.7722	−3.334
	60th cycle	2.6850		2.6798	

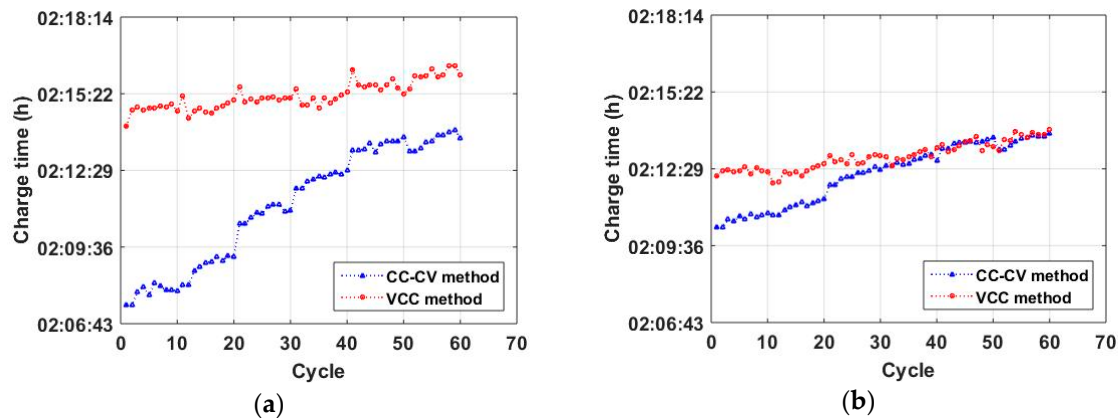


Figure 8. The charge time by cycle number: (a) cell with NCA material; (b) cell with NMC material.

### 7. Conclusion

This paper proposes a variable charging current charging algorithm to minimize the aging characteristics of batteries generated by repeated charging/discharging operation. The proposed method is to manage heat inside the battery that occurs when charging the battery to minimize the battery aging caused by repeated use of the battery. For heating management of batteries, the charging current is varied at each SOC level depending on the internal resistance value of the battery to maintain the power loss inside the battery. The effectiveness of the proposed charging algorithm was then compared with that of the conventional CC-CV charging algorithm. By applying the proposed algorithm, a battery with repeated charging would have a slower aging effect compared to a battery with the conventional charging method. Also, the effects of the proposed algorithm vary depending on the chemical composition of the battery and the proposed algorithm was found to be more effective in high-power battery cells. Based on the results of this experiment, the variable charging current battery charging algorithm proposed in this paper is an effective charging method that slows down the

aging of the battery, and is expected to achieve better results in applications where the product has a long life cycle and battery replacement is difficult. Further research to compare the results of battery aging through long-term charging cycle testing and to adjust charging current to reflect the changes in capacity due to aging of batteries should be carried out.

**Author Contributions:** Conceptualization, I.-H.C. and J.-H.K.; methodology, I.-H.C.; validation, I.-H.C., P.-Y.L. and J.-H.K.; formal analysis, I.-H.C., P.-Y.L. and J.-H.K.; investigation, I.-H.C., P.-Y.L. and J.-H.K.; data curation, P.-Y.L.; writing—original draft preparation, I.-H.C.; writing—review and editing, I.-H.C. and J.-H.K.

**Funding:** This research was supported by a grant from the R&D Program (No. PK1904B1C) of the Korea Railroad Research Institute, Republic of Korea.

**Conflicts of Interest:** The authors declare no conflict of interest.

## References

- Petzi, M.; Kasper, M.; Danzer, M.A. Lithium plating in a commercial lithium-ion battery—A low-temperature aging study. *J. Power Sources* **2015**, *275*, 799–807. [[CrossRef](#)]
- Vetter, J.; Novak, P.; Wagner, M.R.; Veit, C.; Moller, K.C.; Besenhard, J.O.; Winter, M.; Wohlfahrt-Mehrens, M.; Vogler, C.; Hammouch, A.; et al. Ageing mechanisms in lithium-ion batteries. *J. Power Sources* **2005**, *147*, 269–281. [[CrossRef](#)]
- Lee, J.H.; Lee, H.M.; Ahn, S. Battery dimensional changes occurring during charge/discharge cycles—Thin rectangular lithium ion and polymer cells. *J. Power Sources* **2003**, *119–121*, 833–837. [[CrossRef](#)]
- Wu, C.; Zhu, C.; Ge, Y.; Zhao, Y. A review on fault mechanism and diagnosis approach for Li-ion batteries. *J. Nanomater.* **2015**, *2015*, 8. [[CrossRef](#)]
- Belov, D.; Yang, M.H. Failure Mechanism of Li-ion Battery at Overcharge Condition. *J. Solid State Electrochem.* **2008**, *12*, 885–894. [[CrossRef](#)]
- Timmermans, J.M.; Nikolian, A.; De Hoog, J.; Gopalakrishnan, R.; Goutam, S.; Omar, N.; Coosemans, T.; Van Mierlo, J.; Warnecke, A.; Sauer, D.U.; et al. Batteries 2020—Lithium-ion battery first and second life ageing, validated battery models, lifetime modelling and ageing assessment of thermal parameters. In Proceedings of the 2016 18th European Conference on Power Electronics and Applications, Karlsruhe, Germany, 5–9 September 2016.
- Keil, P.; Jossen, A. Charging protocols for lithium-ion batteries and their impact on cycle life—An experimental study with different 18650 high-power cells. *J. Energy Storage* **2016**, *6*, 125–141. [[CrossRef](#)]
- Zhang, S.S. The effect of the charging protocol on the cycle life of a Li-ion battery. *J. Power Sources* **2006**, *161*, 1385–1391. [[CrossRef](#)]
- Guo, Z.; Liaw, B.Y.; Qiu, X.; Gao, L.; Zhang, C. Optimal charging method for lithium ion batteries using a universal voltage protocol accommodating aging. *J. Power Sources* **2015**, *274*, 957–964. [[CrossRef](#)]
- Zheng, J.; Engelhard, M.H.; Mei, D.; Jiao, S.; Polzin, B.J.; Zhang, J.G.; Xu, W. Electrolyte additive enabled fast charging and stable cycling lithium metal batteries. *Nat. Energy* **2017**, *2*, 17012. [[CrossRef](#)]
- Liu, Y.H.; Luo, Y.F. Search for an optimal rapid-charging pattern for li-ion batteries using the Taguchi approach. *IEEE Trans. Ind. Electron.* **2010**, *57*, 3963–3971. [[CrossRef](#)]
- Botsford, C.; Szczepanek, A. Fast Charging vs. Slow Charging: Pros and cons for the New Age of Electric Vehicles. In Proceedings of the Evs24 International Battery, Hybrid and Fuel Cell Electric Vehicle Symposium, Stavanger, Norway, 13–16 May 2009.
- Ikeya, T.; Sawada, N.; Murakami, J.I.; Kobayashi, K.; Hattori, M.; Murotani, N.; Ujiie, S.; Kajiyama, K.; Nasu, H.; Narisoko, H.; et al. Multi-step constant-current charging method for an electric vehicle nickel/metal hydride battery with high-energy efficiency and long cycle life. *J. Power Sources* **2002**, *105*, 6–12. [[CrossRef](#)]
- Gol, E.; Heidary, M.; Kojabadi, H.M. Comparison of Different Battery Charging Methods for Sustainable Energy Storing Systems. In Proceedings of the 26th International Power Systems Conference, Tehran, Iran, 31 October 2011.
- Min, H.; Sun, W.; Li, X.; Guo, D.; Yu, Y.; Zhu, T.; Zhao, Z. Research on the optimal charging strategy for Li-ion batteries based on multi-objective optimization. *Energies* **2017**, *10*, 709. [[CrossRef](#)]

16. Yilmaz, M.; Krein, P.T. Review of charging power levels and infrastructure for plug-in electric and hybrid vehicles. In Proceedings of the 2012 IEEE International Electric Vehicle Conference, Greenville, SC, USA, 4–8 March 2012.
17. Shen, W.; Vo, T.T.; Kapoor, A. Charging algorithms of lithium-ion batteries: An overview. In Proceedings of the 2012 7th IEEE Conference on Industrial Electronics and Applications, Singapore, 18–20 July 2012.
18. Shirk, M.; Wishart, J. Effects of Electric Vehicle Fast Charging on Battery Life and Vehicle Performance. *SAE Tech. Paper 2015-01-1190* **2015**. [[CrossRef](#)]
19. Kettles, D. *Electric Vehicle Charging Technology Analysis and Standards*; FSEC-CR-1996-15; Florida Solar Energy Center: Cocoa, FL, USA, February 2015.
20. Wang, D.; Bao, Y.; Shi, J. Online Lithium-Ion Battery Internal Resistance Measurement Application in State-of-Charge Estimation Using the Extended Kalman Filter. *Energies* **2017**, *10*, 1284. [[CrossRef](#)]
21. Ecker, M.; Gerschler, J.B.; Vogel, J.; Käbitz, S.; Hust, F.; Dechent, P.; Sauer, D.U. Development of a lifetime prediction model for lithium-ion batteries based on extended accelerated aging test data. *J. Power Sources* **2012**, *215*, 248–257. [[CrossRef](#)]
22. Fleischhammer, M.; Waldmann, T.; Bisle, G.; Hogg, B.I.; Wohlfahrt-Mehrens, M. Interaction of cyclic ageing at high-rate and low temperatures and safety in lithium-ion batteries. *J. Power Sources* **2015**, *274*, 432–439. [[CrossRef](#)]
23. Liaw, B.Y.; Roth, E.P.; Jungst, R.G.; Nagasubramanian, G.; Case, H.L.; Doughty, D.H. Correlation of Arrhenius behaviors on power and capacity fades, impedance, and static heat generation in lithium ion cells. *J. Power Sources* **2003**, *119*, 874–886. [[CrossRef](#)]
24. Onda, K.; Ohshima, T.; Nakayama, M.; Fukuda, K.; Araki, T. Thermal behavior of small lithium-ion battery during rapid charge and discharge cycles. *J. Power Sources* **2006**, *158*, 535–542. [[CrossRef](#)]
25. Abdollahi, A.; Han, X.; Avvari, G.V.; Raghunathan, N.; Balasingam, B.; Pattipati, K.R.; Bar-Shalom, Y. Optimal battery charging, Part 1: Minimizing time-to-charge, energy loss, and temperature rise for OCV-resistance battery model. *J. Power Sources* **2016**, *303*, 388–398. [[CrossRef](#)]
26. FreedomCAR Battery Test Manual for Power-Assist Hybrid Electric Vehicles. Available online: [https://avt.inl.gov/sites/default/files/pdf/battery/freedomcar\\_manual\\_04\\_15\\_03.pdf](https://avt.inl.gov/sites/default/files/pdf/battery/freedomcar_manual_04_15_03.pdf) (accessed on 22 June 2019).
27. Seaman, A.; Dao, T.-S.; McPhee, J. A survey of mathematics-based equivalent-circuit and electrochemical battery models for hybrid and electric vehicle simulation. *J. Power Sources* **2014**, *256*, 410–423. [[CrossRef](#)]
28. Lai, X.; Zheng, Y.; Sun, T. A comparative study of different equivalent circuit models for estimating state-of-charge of lithium-ion batteries. *Electrochim. Acta* **2017**, *259*, 566–577. [[CrossRef](#)]
29. Qian, K.; Huang, B.; Ran, A.; He, Y.B.; Li, B.; Kang, F. State of health (SOH) evaluation on lithium ion battery by simulating the voltage relaxation curves. *Electrochim. Acta* **2019**, *303*, 183–191. [[CrossRef](#)]
30. Kwon, S.J.; Lee, S.E.; Lim, J.H.; Choi, J.H.; Kim, J.H. Performance and Life Degradation Characteristics Analysis of NCM LIB for BESS. *Electronics* **2018**, *7*, 406. [[CrossRef](#)]
31. Lu, Z.; Yu, X.L.; Wei, L.C.; Cao, F.; Zhang, L.Y.; Meng, X.Z.; Jin, L.W. A comprehensive experimental study on temperature-dependent performance of lithium ion battery. *Appl. Therm. Eng.* **2019**, *158*, 113800. [[CrossRef](#)]
32. Yang, J.; Xia, B.; Huang, W.; Fu, Y.; Mi, C. Online state of health estimation for lithium ion batteries using constant voltage charging current analysis. *Appl. Energy* **2018**, *212*, 1589–1600. [[CrossRef](#)]

